

Fluorinated networks dynamics studied by means of broadband dielectric spectroscopy

Luis A. Miccio,^{1,2,3} Jon Otegui,¹ Marcela E. Penoff,⁴ Pablo E. Montemartini,⁴ Gustavo A. Schwartz^{1,2}

¹Centro de Física de Materiales (CSIC-UPV/EHU), P. M. de Lardizabal 5, San Sebastian 20018, Spain

²Donostia International Physics Center, P. M. de Lardizabal 4, San Sebastian 20018, Spain

³Departamento de Física de Materiales (UPV/EHU), San Sebastian 20080, Spain

⁴Instituto de Investigación en Ciencia y Tecnología de Polímeros (INTEMA), Mar del Plata, Argentine

Correspondence to: L. A. Miccio (E-mail: luisalejandro_miccio@ehu.es)

ABSTRACT: The influence of the surface chemical modification on the bulk behavior of epoxy based networks has been studied. In particular, the bulk dynamics of epoxy-amine networks modified with fluorinated side chains has been characterized by means of broadband dielectric spectroscopy (BDS), differential scanning calorimetry (DSC) and Fourier transform infrared (FTIR) spectroscopy. The fluorination effect on the structure and dynamics of the materials has been related with the observed changes in both segmental and secondary relaxations. An acceleration of the segmental dynamics as the fluorination degree increases has been clearly observed. As a result, a compromise between fluorine surface enrichment and bulk modification has been proposed for these materials. © 2015 Wiley Periodicals, Inc. *J. Appl. Polym. Sci.* **2015**, *132*, 42690.

KEYWORDS: coatings; composites; crosslinking; functionalization of polymers; surfaces and interfaces

Received 13 January 2015; accepted 29 June 2015

DOI: 10.1002/app.42690

INTRODUCTION

Fluorine-containing materials are generally used as engineering plastics and high-tech elastomers. They also find considerable application in the coatings industry because of their excellent surface properties like water and oil repellency, low coefficient of friction, and high chemical resistance. However, the synthesis and high costs of these fluorinated materials together with the additional intrinsic processing problems have limited their application to niche segments of the market. Fluorinated surfaces derive their characteristics from the C—F bond that grants a specific, unique chemistry to the materials. It is well known that the low surface free energy of a component provides a thermodynamic driving force for migration to interfaces.^{1–7} Due to this natural migration it is possible to design materials with controlled surface properties by employing a low content of the expensive modifier and, at the same time, by discarding processing problems related to high fluorine concentrations.

Fluorine has been introduced in many types of polymers, such as polyurethanes, polymethacrylates, styrene and epoxies, to name a few.^{1,2,5,7,8} Among these polymers, epoxy resin based materials exhibit outstanding properties which make them a standard option for many applications such as adhesives, coat-

ings, and structural composites. One of their most attractive features is the flexibility in the election of their monomers and co-monomers, which in turn leads to a wide variety of products, i.e. from low T_g rubbers to high T_g materials. Furthermore, their chemical structure can be modified to attain different properties, i.e., to increase the toughness, or to obtain a functional polymer. In this sense, the incorporation of low surface energy compounds appears as a very interesting approach for obtaining materials with high hydrophobicity, low friction, and low dielectric constant.

In the design of materials for industrial applications, the fulfillment of several requirements at the same time is in general a requisite i.e: modulus, hardness, chemical and thermal resistance, among others. In particular, reinforced materials for energy industry applications like wind turbine blades or oil pipes is especially challenging. In the former case, the efficiency of wind farms strongly decreases as ice and dirt sticks to the wind turbine blades (fouling). On the other hand, time growing paraffin deposits continuously reduce the flux section, and therefore the lifespan of oil pipes. As a result, it is desirable to obtain a synergetic combination of the outstanding surface properties of fluorinated polymers with the mechanical properties of the epoxy matrix of these reinforced materials.

Additional Supporting Information may be found in the online version of this article.

© 2015 Wiley Periodicals, Inc.

The key factors determining the behavior of the reinforced materials are the individual properties of both filler and matrix, and the filler–polymer interaction. In this sense, with the aim of modifying the epoxy matrix, it is necessary to determine the extent and the nature of this modification. While surface properties have been extensively studied, to the point of being the motivation of the here proposed chemical modification, the fluorine side effects in the bulk network behavior have not yet been fully characterized. As the polymer dynamics is sensitive to the matrix structure and the presence of the filler, these studies can be performed by using mechanical, i.e., rheometry; or electrical approaches, i.e., broadband dielectric spectroscopy (BDS). In particular, BDS has shown to be a very useful technique in the study of the molecular dynamics of insulating materials. The huge frequency range achieved (10^{-5} – 10^{12} Hz) and the possibility of measuring under different temperature, pressure, and environmental conditions, allows the observation of a large variety of processes with very different time scales. Within this extraordinary experimental window, molecular and collective dipolar fluctuations, charge transport and polarization effects take place, in turn determining the dielectric response of the material under study.⁹ Therefore, BDS can yield information about the dynamics of the polymer backbone, pendant chains and lateral groups both macroscopically^{10,11} and microscopically.^{12–15}

In this work, we study the dynamics of fluorinated epoxy-amine networks, to determine the changes produced by the chemical modification in comparison with the unmodified material. We use a combination of BDS with calorimetric information obtained through differential scanning calorimetry (DSC) and chemical structure information from Fourier transform infrared spectroscopy (FTIR). In a first step, we characterize the monomers involved in the synthesis, along with the intermediate fluorinated oligomer. In a second step, we use the previously obtained information to determine the fluorinated modifier influence on the network properties.

MATERIALS AND METHODS

Materials

Polymer networks with different fluorine content were synthesized by following a two step procedure:

- Reaction of a perfluorinated epoxy (2,2,3,3,4,4,5,5,6,6,7,7,8,9,9,9-hexadecafluoro-8-trifluoromethyl nonyloxirane, FED3, Sigma-Aldrich) with a known excess of a di-amine (propyleneoxidediamine, Jeff, Huntsman). The reaction was performed in sealed tubes immersed in an oil bath, whose temperature was kept at 100°C for 120 min. In this step the fluorinated epoxy chemically bonds to the di-amine, therefore producing a small quantity of a fluorinated amine within a large amount of unreacted Jeff (for additional information see Supporting Information Figure S1). The fluorination degree in the final materials was controlled by varying the ratio of fluorinated epoxy to amino-hydrogen groups in this step.
- Reaction of the remaining amine groups with a stoichiometric amount (ratio of epoxy to amino-hydrogen groups equal to 1) of a difunctional epoxy (diglycidyl ether of bisphenol

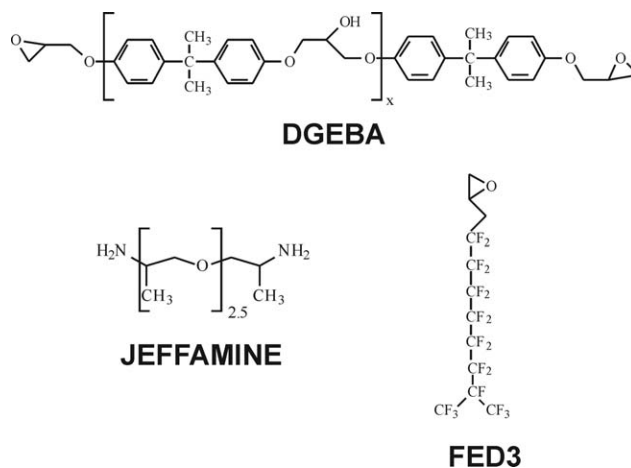


Figure 1. Chemical structure of the reactants.

A, DGEBA). The temperature during the curing reaction was kept at 100°C for the time necessary to obtain total conversion of the reactants, in the presence of 10 wt % of Toluene.^{4–6} The so obtained fluorinated networks are solid disks with a diameter of 40 mm and a thickness of about 0.7 mm. The materials containing from 0 to 5 wt % F were called FE0 to FE5, respectively. Figure 1 shows the structure of the above mentioned reactants.

A fluorinated oligomer obtained from the reaction of FED3 and Jeff, fluorinated Jeff (JMF) was also studied to facilitate the identification of the experimentally observed relaxation processes. JMF was synthesized by using step “a” conditions, and a ratio of epoxy to amino-hydrogen groups equal to 4.^{4–6}

DSC Experimental Setup

DSC measurements were performed using a DSC Q2000 from TA Instruments. Samples of about 10 mg were sealed in hermetic aluminum pans. Heating–cooling cycles were performed under nitrogen flow in the temperature range from –125 to 150°C, with a heating/cooling rate of 10°C/min. The annealing time between cooling and heating runs was set to 5 minutes. Glass transition temperature (T_g) was determined at the inflection point of the curves and the heat capacity increment (ΔC_p) was estimated from the difference in the heat capacity value extrapolation after and before T_g (second runs were taken to delete any effects of thermal history).

FTIR Experimental Setup

FTIR spectroscopy was performed using a FTIR Thermo Scientific Nicolet 6700 and a Genesis II Matson spectrometers. Temperature measurements were performed using a heated transmission cell (HT-32, Spectra Tech) and a programmable temperature controller (Omega, Spectra Tech, $\Delta T = \pm 1^\circ\text{C}$). Near-infrared spectroscopy (NIR), 7000–4000 cm^{-1} , was used to determine polymerization kinetics. All spectra were collected with 8 cm^{-1} resolution and 24 scans per slice. The sample was placed between two glasses using a 1 mm rubber spacer. The temperature during the polymerization kinetics was kept constant at 100°C. The peaks at 4538 cm^{-1} (assigned to the conjugated epoxy CH_2 deformation band with the aromatic CH fundamental stretch)¹⁶ and at 4940 cm^{-1} ¹⁷ (primary amine

combination band), were used to monitor the disappearance of the epoxy group and the primary amine, respectively. Both peaks were normalized to the reference band at 5056 cm^{-1} (phenyl combination band)¹⁸ for reactions involving DGEBA monomer, and at 4334 cm^{-1} (CH_2 combination band)¹⁸ for reactions involving Jeff.

BDS Experimental Setup

Broadband dielectric spectroscopy measurements were performed on disc shaped samples with a diameter of 40 mm and a thickness of about 0.7 mm. The samples were placed between two parallel-plate electrodes. For parallel-plate configuration, the sample capacitance is expressed as $C = \epsilon \epsilon_0 A/d$, where ϵ is the relative dielectric permittivity of the sample, ϵ_0 the vacuum permittivity, A is the section of the sample, and d its thickness. The material properties are characterized by the complex dielectric permittivity, ϵ^* , which is defined as $\epsilon^*(\omega) = C^*(\omega)/C_0 = \epsilon'(\omega) - i \epsilon''(\omega)$, where C_0 is the capacitance of the empty capacitor and $\omega = 2\pi f$. A broadband high-resolution dielectric spectrometer (Novocontrol Alpha) was used to measure the complex dielectric permittivity in the frequency range from 10^{-2} to 10^6 Hz. The sample temperature was controlled by nitrogen gas flow that provides temperature stability of about ± 0.1 K (Quattro temperature controller).

RESULTS AND DISCUSSION

Reactants Characterization

To identify the origin of each observed relaxation process in the fluorinated networks, we characterized all the reactants involved in their synthesis. With this aim, DSC, FTIR and BDS experiments were also conducted.

β and γ Relaxation. Figure 2 shows the isothermal dielectric loss spectra for Jeff (pink triangles), FED (orange circles) and DGEBA (black squares) at 160 K and 185 K. At low temperatures, two relaxation processes can be observed for the analyzed reactants: (1) α (segmental) and γ (secondary) relaxations for Jeff and FED (although only one secondary relaxation is observed, for clarity purposes it has been called γ), and (2) β and γ secondary relaxations for DGEBA. Above T_g the cooperative movement of the chains segments produces the α -relaxation process for Jeff [see Figure 2(a)] and FED [see Figure 2(a,b)]. On the other hand, in this temperature range DGEBA is still in the glassy state where the cooperative movements are frozen.

Jeff α -relaxation overlaps the corresponding γ relaxation process, therefore impeding an accurate analysis when the temperature is increased. FED spectra also present difficulties for the fitting due to the fact that α and γ processes are overlapped at low temperatures, as shown in Figure 2(a). Although both processes shift to higher frequencies as the temperature is increased, the temperature dependence of the α -relaxation is stronger, thus overlapping the γ process. To study these processes, the γ relaxation was individually characterized at very low temperatures (where α process is outside of the experimental frequency window) and the α process was then fitted at higher temperatures (by extrapolating and fixing the previously obtained γ parameters).

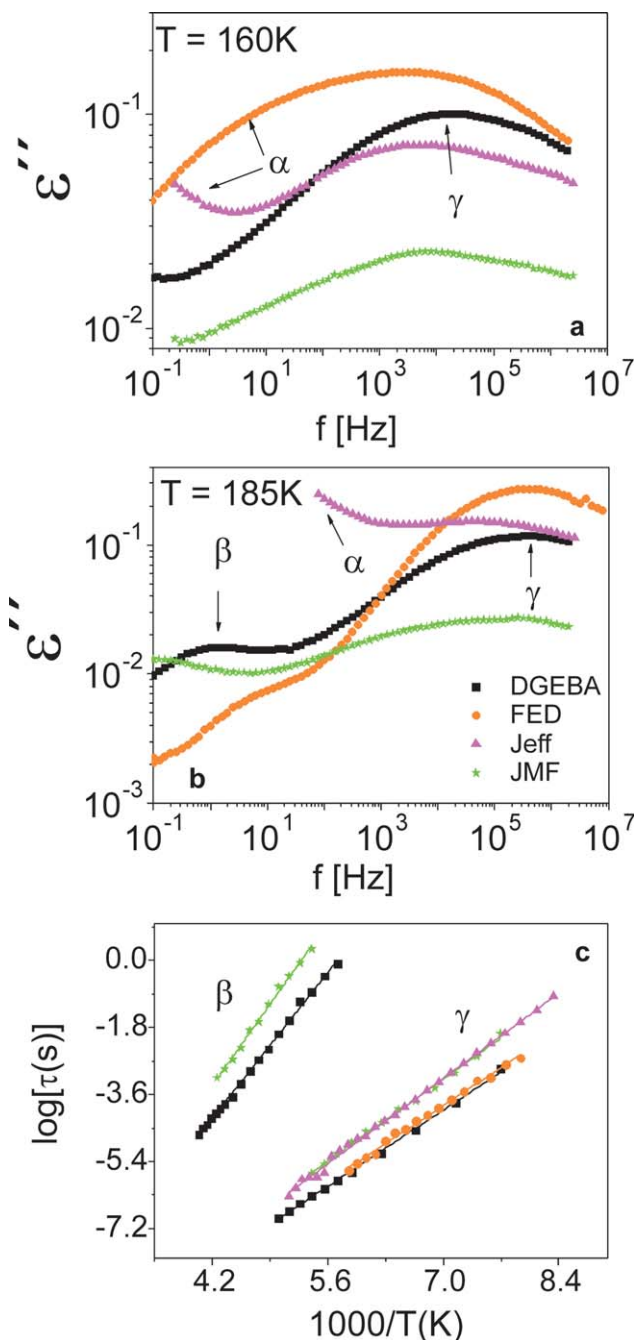


Figure 2. Isothermal dielectric loss spectra for reactants and JMF at (a) 160 K and (b) 185 K (c) Corresponding relaxation map (the dots stand for the experimental points and the lines for the fitting). [Color figure can be viewed in the online issue, which is available at wileyonlinelibrary.com.]

At low temperatures, where DGEBA is in the glassy state, two peaks corresponding to the β and γ secondary relaxations are observed. The β relaxation is around five orders of magnitude slower than the γ process (i.e. the groups responsible of the γ process possess a much higher mobility). In addition, the dielectric intensity of the β process is significantly lower than that of the γ process.

As already explained in Materials section, during the first synthesis step of the fluorinated networks, an epoxy-amine addition

Table I. BDS Fitting Parameters and Glass Transition Temperatures Obtained by DSC for the Reactants

Sample	VFT parameters			m	T_{g100s} (K)	$E_{\alpha\beta}$ (kJ/mol)	$E_{\alpha\gamma}$ (kJ/mol)	T_g (K)
	$\log\tau_0$	T_0 (K)	D					
FED	-11.8 ± 0.4	131.4 ± 1.4	4.2 ± 0.4	117.6	148.8	-	27.8 ± 0.5	152.35
DGEBA	-14.1 ± 0.4	220.4 ± 1.9	5.9 ± 0.5	117.1	255.5	53.6 ± 0.5	28.0 ± 0.3	258
Jeff	-12.8 ± 0.1	152.0 ± 0.5	6.7 ± 0.2	90.1	181.8	-	30.5 ± 0.1	184.9
JMF	-13.5 ± 0.3	175.1 ± 3.2	12.0 ± 1.1	61.7	233.9	59.7 ± 1.3	30.1 ± 0.5	239

$\log\tau_0$, T_0 , and D were obtained from the fitting of the BDS data by using a Vogel-Fulcher-Tammann (VFT) equation. The extrapolation to a relaxation time of $\tau = 100$ s gives a dielectric estimation of the glass transition temperature (T_{g100s}).²⁷ $E_{\alpha\beta}$ and $E_{\alpha\gamma}$ stand for the activation energies obtained from the Arrhenius temperature dependence of the relaxation time for the secondary processes β and γ . T_g stands for the calorimetric glass transition temperature as obtained from DSC measurements.

reaction between the fluorinated epoxy (FED) and the diamine (Jeff) is carried out. As a result, the fluorinated oligomer is attached to the Jeff molecule (and later to the epoxy-amine network in the final materials) as a pendant chain. To identify the relaxation processes related with these pendant chains another oligomer was introduced in the analysis, JMF.^{2,4,5} Like DGEBA, JMF is in the glassy state at the temperatures shown in Figure 2, and therefore only β and γ secondary relaxations are observed. Both position and shape of the γ process in JMF are similar to its Jeff counterpart (this could be a clue in the identification of the γ process for JMF and Jeff).

For the analysis of β and γ relaxation processes, the dielectric loss spectra, $\epsilon''(f)$, was fitted by using a Cole-Cole equation (CC)^{9,19} which is commonly used to describe this kind of symmetric peaks.

$$\epsilon''(\omega) = \epsilon_\infty + \frac{\Delta\epsilon}{1 + (i\omega\tau_{cc})^\alpha} \quad (1)$$

where τ_{cc} is the CC relaxation time, $\Delta\epsilon$ is the relaxation strength, α is a shape parameter ($0 < \alpha \leq 1$) and ω is the angular frequency. Figure 2(c) shows the corresponding relaxation map for β and γ processes for the different reactants and JMF. As expected, the relaxation times for both secondary relaxations follow an Arrhenius behavior [$\tau = \tau_0 \cdot e^{E_a/kT}$] in the temperature range here analyzed. The corresponding activation energies (E_a) were obtained from the slope of the Arrhenius fittings on the relaxation map (see Table I). The temperature dependence of the relaxation times for the γ processes in DGEBA and FED are identical; both overlap along the analyzed temperature range (presenting the same activation energy values). Therefore, it is reasonable to assume that the same group is involved in these relaxations, i.e., epoxy group.²⁰⁻²² A similar behavior is observed for the γ relaxation of both Jeff and JMF (where the relaxation times and activation energies also coincide). In addition, FTIR spectroscopy was employed to help in the identification of these dielectric signals through the analysis of the chemical species within the material.

Figure 3 presents the corresponding FTIR spectra for all the above mentioned reactants. As expected, both DGEBA and FED present prominent epoxy related signals¹⁸ [see Figure 3(b,c), respectively]. Hence, these spectra further support the previous assumptions concerning to the origin of the observed γ relaxations (for further information see Supporting Information Table S1).

As shown in Figure 3(a), JMF does not have any residual epoxy groups, but in turn it conserves both Jeff and FED backbones. Figure 2(c) clearly shows that JMF γ relaxation process position does not change with respect to the original Jeff one. Therefore, it is reasonable to assume that this process is related to a group belonging to the Jeff molecule and not to the presence of the fluorinated pendant chain. By considering all the dipoles (having a strong dielectric signal) in Jeff molecule, and by taking into account the proximity of this process to that of the epoxy group (in turn observed in FED and DGEBA), ether appears as the most suitable responsible of the observed relaxation.^{20,21} Figure 4 shows FTIR spectra in both mid and near infrared

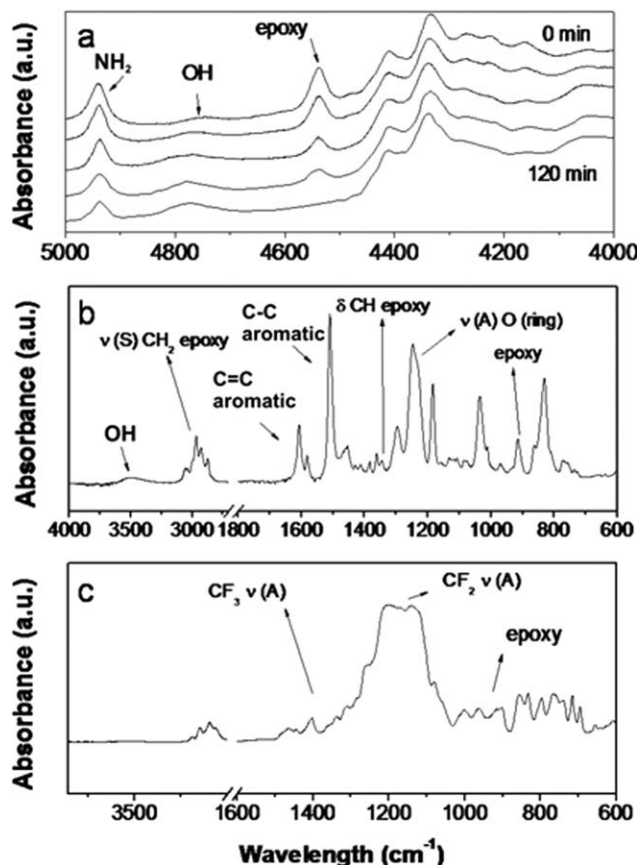


Figure 3. FTIR spectra of (a) Equimolar mixture of Jeffamine D230 and FED3 reacting at 100°C for 120 min, (b) DGEBA, (c) FED3.

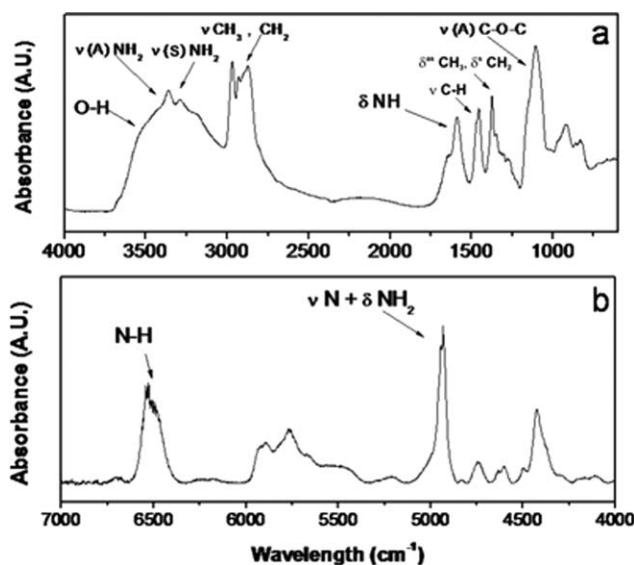


Figure 4. FTIR spectra in both mid (a) and near (b) infrared ranges for Jeffamine D230.

ranges for Jeff, where ether related signals can be clearly identified.

Concerning to the observed β relaxation in JMF and DGEBA, FTIR experiments were also used to obtain complementary information of their origin. Therefore, it is possible to observe the presence of OH groups in both JMF and DGEBA, as clear signals at about 4750 cm^{-1} and 3500 cm^{-1} in the corresponding spectra [see Figure 3(a,b)]. In the first case, these OH groups are originated during the epoxy-amine reaction. As shown in Figure 3(a), at higher reaction times the OH signal strength increases while its epoxy counterpart decreases (the epoxy-amine addition reaction is shown in Figure 5). In the second case, OH groups in DGEBA are originally present in the molecule backbone. The differences in the observed OH relaxations could be interpreted as an evidence of a different dielectric environment.

α Relaxation. At temperatures close to the calorimetric glass transition of the reactants, a broad loss peak (in some cases two orders of magnitude stronger than the secondary β and γ loss peaks) steps into the experimental frequency window upon increasing temperature. This peak is recognized as the segmental or α relaxation processes. For the analysis of these α relaxation processes, the dielectric loss spectra, $\varepsilon''(f)$, was fitted by using a Havriliak-Negami function (HN),²³ which accounts for the asymmetric broadening typically observed for the α -process.

$$\varepsilon^*(\omega) = \varepsilon_{\infty} + \frac{\Delta\varepsilon}{[1 + (i\omega\tau_{HN})^{\alpha}]^{\beta}} \quad (2)$$

Besides the parameters previously described in (1), an additional β shape parameter describing the α -relaxation asymmetry



Figure 5. Epoxy-amine addition reaction scheme.

is introduced in this equation. In addition, the temperature dependence of the α -process relaxation time (τ_{HN}) can be well described by the Vogel-Fulcher-Tammann (VFT) equation.

$$\tau(T) = \tau_0 \cdot e^{\frac{D \cdot T_0}{T - T_0}} \quad (3)$$

where τ_0 is the reciprocal of a characteristic vibrational frequency, T_0 is the temperature at which the extrapolated relaxation time tends to diverge, and D is connected with the so-called fragility strength parameter.^{9,24–26} The extrapolation to a relaxation time of $\tau = 100\text{ s}$ gives a dielectric estimation of the glass transition temperature (T_{g100s}).²⁷ Figure 6 shows the relaxation map of the α process for each of the above mentioned reactants and JMF. As expected, the pendant fluorinated chain attached to the Jeff molecule affects the relaxation time of JMF (substantially larger than the observed Jeff relaxation time). As already mentioned, FED α relaxation is the fastest among the reactants, up to the point that it is overlapped with the relaxation of the epoxy group in the molecule.

As shown in Table I, calorimetric and dielectric data present the same trend, with T_{g100s} always 3 or 4 degrees higher than their calorimetric counterparts. This situation is often encountered in chain dynamics studies in polymeric systems and is sometimes explained in terms of the different nature of DSC (static) and dielectric ways of determining T_g .⁹ (DSC data can be observed in Supporting Information Figure S2).

Networks Characterization

With the information about dielectric relaxations obtained for the individual reactants, it is now possible to analyze the dynamics of the epoxy-amine networks. Therefore, in this section the dynamics of epoxy compounds with different amounts of flexible fluorinated chains is studied in detail. As in the case of the reactants, DSC, FTIR and BDS experiments were carried out. The broad frequency and temperature ranges covered by BDS allow the study of all the relaxation processes occurring in the samples: from local motions (β and γ secondary relaxations) at low temperatures/high frequencies, to cooperative segmental motions (α -relaxation) at high temperatures/low frequencies. Table II

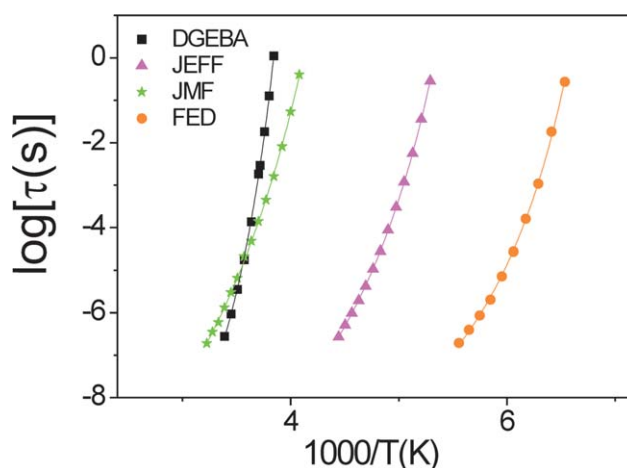


Figure 6. Relaxation map of the α processes for reactants and JMF. [Color figure can be viewed in the online issue, which is available at wileyonlinelibrary.com.]

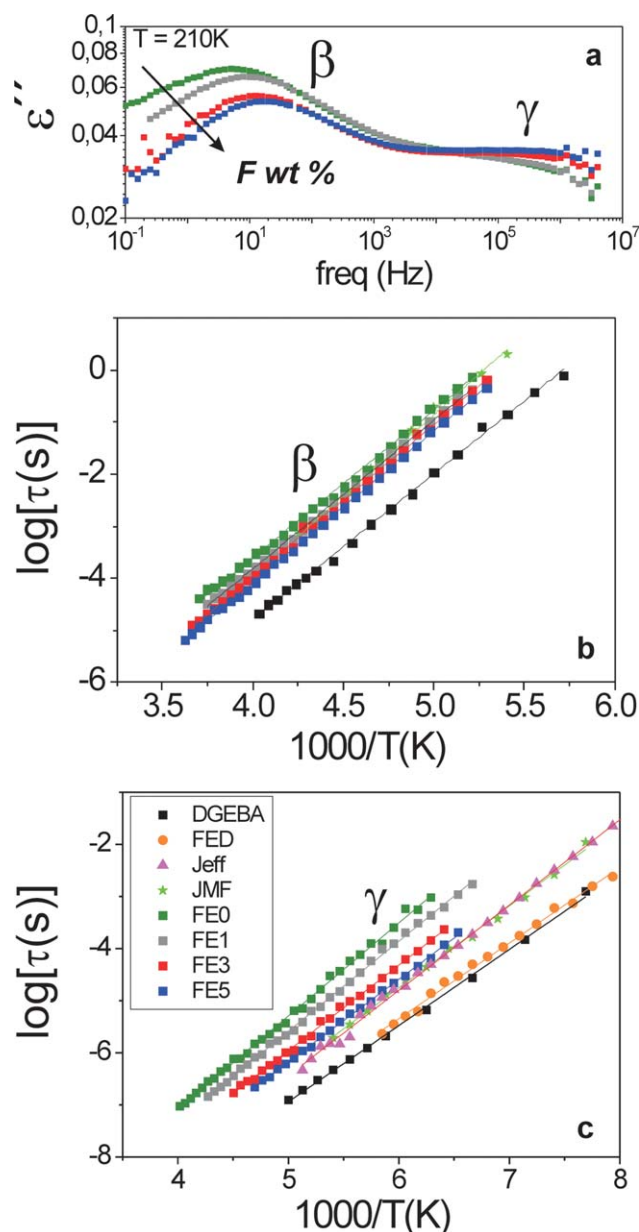


Figure 7. (a) Isothermal dielectric loss spectra for fluorinated networks at 210 K. (b) Corresponding relaxation map for the β relaxation process. (c) Corresponding relaxation map for the γ relaxation process (the dots stand for the experimental points and the lines for the fitting). [Color figure can be viewed in the online issue, which is available at wileyonlinelibrary.com.]

shows the Arrhenius and VFT fittings parameters together with the calorimetric T_g -s obtained by DSC.

β and γ Relaxation. Figure 7 shows the comparative isothermal dielectric loss spectra at 210 K and the corresponding relaxation maps for the fluorinated epoxy networks under investigation. In this range of temperatures it is possible to observe two secondary relaxations, β and γ . Both relaxations follow a well-defined trend: as the fluorine content increases the relaxation time of the β and γ -processes decreases. Concerning to the dielectric intensity, two opposite behaviors are observed: (1) the intensity of the β relaxation decreases as the fluorine content increases

and, (2) the intensity of the γ relaxation increases as the fluorine content increases.

As β and γ processes appear in the pure epoxy network (0 wt % FED), their origin may reside either in Jeff or in DGEBA. In this sense, epoxy groups in DGEBA and FED, and ether groups in Jeff, are the most dielectrically active species of their corresponding molecules, as shown in “Reactants Characterization” section. Therefore, epoxy or ether groups could be the responsible for the observed γ relaxation. However, as all the epoxy groups react during the network formation, this relaxation has to be related to the backbone ether groups of the Jeff molecules within the materials. Comparison of the relaxation maps and activation energies ($E_{a\gamma}$) of the materials with Jeff and JMF confirm this hypothesis. Figure 7(c) shows that when the fluorine content increases the relaxation times of γ relaxation decreases, to the point of overlapping their Jeff (and JMF) counterparts. The observed activation energies values are very close to their Jeff and JMF counterparts (see Tables I and II). For FE5, the $E_{a\gamma}$ closely coincides with the Jeff and JMF observed values (30KJ/mol) while for DGEBA and FED the $E_{a\gamma}$ is 28KJ/mol. These

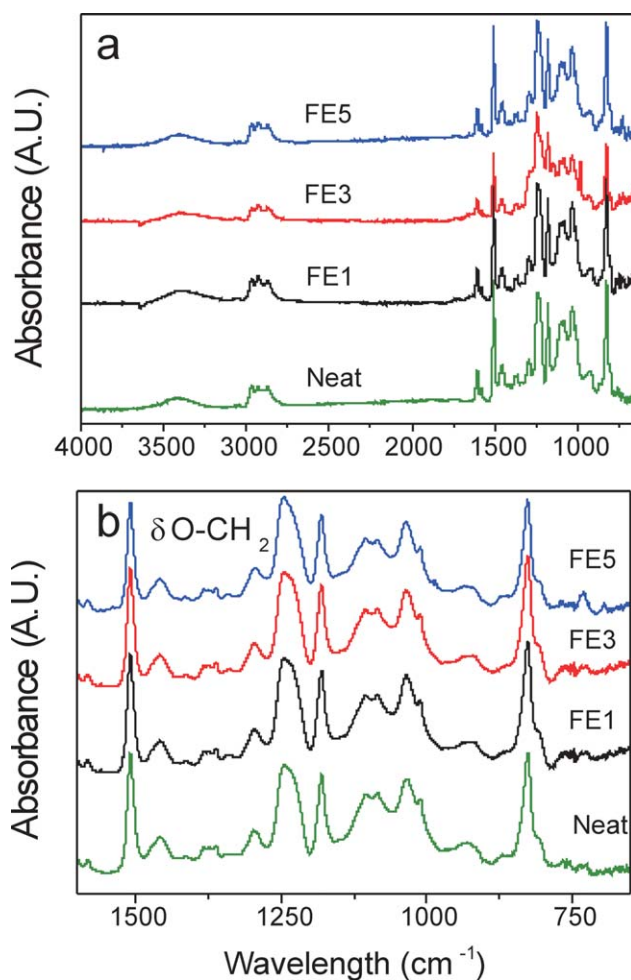


Figure 8. FTIR spectra of the fluorinated networks (a) overall view, (b) zoomed view. [Color figure can be viewed in the online issue, which is available at wileyonlinelibrary.com.]

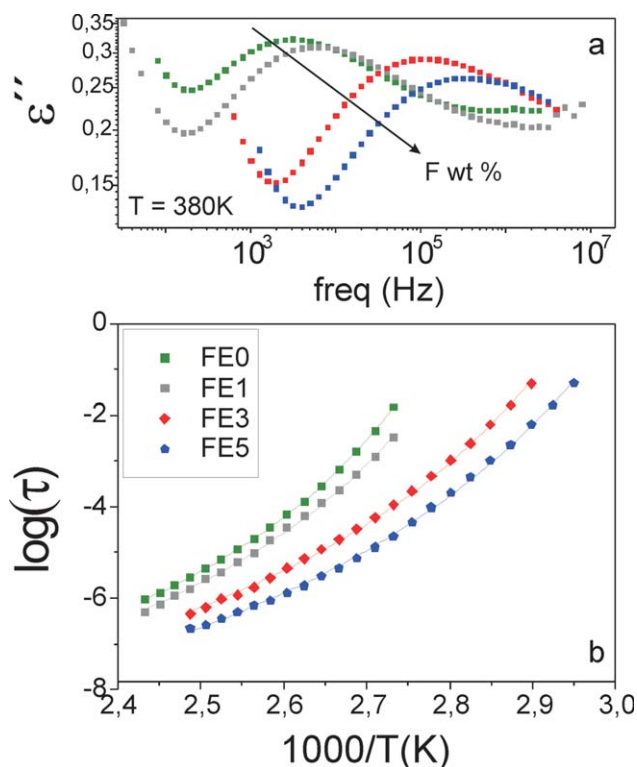


Figure 9. (a) Isothermal dielectric loss spectra for fluorinated networks at 380 K. (b) Corresponding relaxation map for the α relaxation process (the dots stand for the experimental points and the lines for the fitting). [Color figure can be viewed in the online issue, which is available at wileyonlinelibrary.com.]

results further support the association of this process with the ether groups.

On the other hand, the β process of the modified networks is partially overlapped with the corresponding JMF relaxation. This particular relaxation is associated with the OH groups within the molecules, as already pointed out in “Reactants Characterization” section. As commented above, from the BDS spectra [see Figure 7(a)] it is clear that: (1) the relaxation time is shifted to higher frequencies as the fluorine content increases and (2) the intensity of these relaxation peaks decreases as the fluorine content increases. This is probably related to a decrease of the OH concentration due to the fluorine introduction. Every two FED molecules introduced, one DGEBA molecule (and the corresponding attached hydroxyl group) is removed to keep the stoichiometric balance. In addition, $E_{a\beta}$ is unaffected by the fluorine content. Similar values of $E_{a\beta}$ are also obtained for JMF and DGEBA which reinforces the hypothesis that the β secondary relaxation is originated from OH groups (see Table I). FTIR spectra in Figure 8 show the OH signal at about 3500 cm^{-1} (and the absence of unreacted epoxy signals), thus supporting previous statements.

α Relaxation. Glass transition temperatures ranging from 340 to 360 K were found by calorimetry for fluorinated epoxy networks. Similar T_g values were reported also for other epoxy networks using the Jeffamine D230.⁴ A systematic decrease of the T_g is observed by increasing flexible FED chains content in the

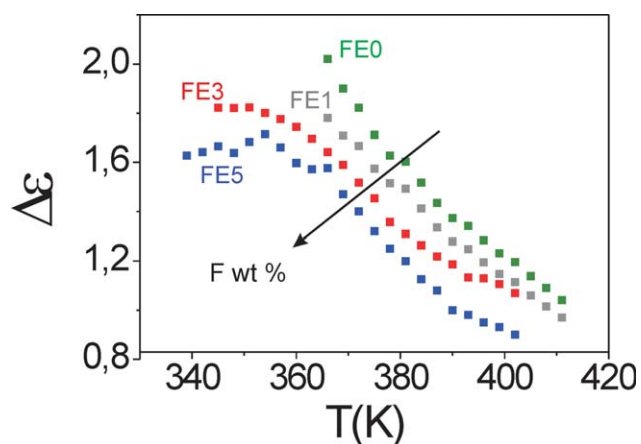


Figure 10. $\Delta\epsilon$ as a function of temperature for fluorinated networks. The dielectric strength values were obtained from the HN [eq. (2)] fitting of the α relaxation. [Color figure can be viewed in the online issue, which is available at wileyonlinelibrary.com.]

networks. Figure 9 shows the dielectric loss spectra of the fluorinated networks obtained at 380 K. The segmental relaxation shifts to higher frequencies as the fluorine content increases, thus indicating an acceleration of the response for the cooperative movements.

Figure 9(b) shows the temperature dependence of the segmental relaxation time for the networks with different fluorine contents and the corresponding VFT fittings (Table II shows the VFT parameters obtained and the calculated T_{g100s}). As the fluorinated materials are obtained from the chemical addition of FED to the diamine, the final networks present pendant flexible chains in their structure. As shown in Figure 10, there is a significant reduction of the relaxation strength in the fluorinated networks, which follow a well defined trend: $\Delta\epsilon$ decreases as the

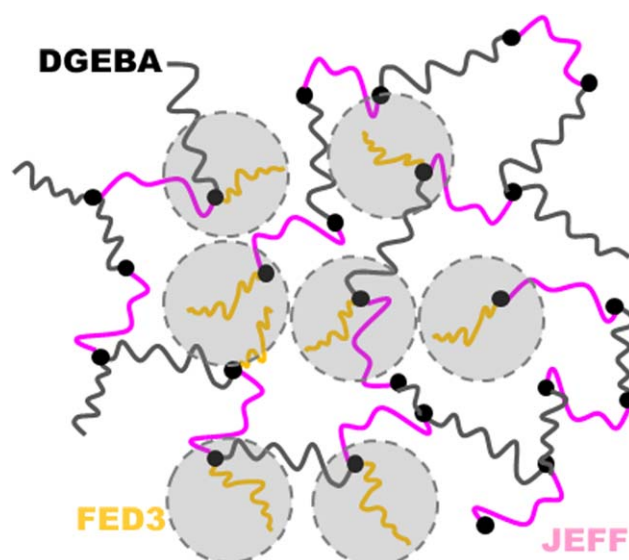


Figure 11. Fluorinated networks scheme (gray circles represent the regions where the crosslink density has been reduced due to the fluorinated chains incorporation). [Color figure can be viewed in the online issue, which is available at wileyonlinelibrary.com.]

Table II. Fitting Parameters for the Temperature Dependence of the Relaxation Times and Glass Transition Temperatures Obtained by DSC for the Modified Networks

Sample	VFT parameters			<i>m</i>	T_{g100s} (K)	$E_{\alpha\beta}$ (kJ/mol)	$E_{\alpha\gamma}$ (kJ/mol)	T_g (K)
	$\log \tau_0$	T_0 (K)	<i>D</i>					
FE0	-10.7 ± 0.1	315.5 ± 0.5	3.3 ± 0.1	124.6	351.2	54.3 ± 0.5	34.2 ± 0.3	358.9
FE1	-10.9 ± 0.1	310.6 ± 1.3	3.5 ± 0.2	122.4	347.2	54.7 ± 0.3	33.1 ± 0.2	354.7
FE3	-11.0 ± 0.2	291.8 ± 3.0	4.1 ± 0.4	108.0	331.8	55.9 ± 0.3	31.4 ± 0.3	348.4
FE5	-11.7 ± 0.2	281.7 ± 2.4	4.9 ± 0.3	101.1	325.6	55.8 ± 0.2	30.3 ± 0.2	339.5

τ_0 is the reciprocal of a characteristic vibrational frequency, T_0 is the temperature at which the extrapolated relaxation time tends to diverge, and *D* is connected with the so-called fragility strength parameter, *m*, through eq. (4).^{9,24-26} T_{g100s} is a dielectric estimation of the glass transition temperature.²⁷ $E_{\alpha\beta}$ and $E_{\alpha\gamma}$ stand for the activation energies of the secondary relaxations β and γ . T_g stands for the calorimetric glass transition temperatures.

fluorine content increases. In addition, a broadening of the dielectric response in the region of the glass transition can be observed with increasing fluorine content. These results suggest an increasing heterogeneity of chain dynamics at glass transition; i. e. the chain dynamics is different in different regions of the sample. According to the Addam-Gibbs framework,²⁸ the characteristic size of these regions must be larger than the size of the cooperative rearrangement region (CRR), which has been determined for various polymers to be in the range 1–4 nm by means of mechanical,^{29,30} dielectric,^{31,32} and calorimetric^{33,34} methods. The spatial heterogeneity in the networks can be understood in terms of increasing free volume due to loosened molecular packing of the networks.

Rationalization of Results

BDS and DSC results show that the α relaxation becomes systematically faster as the fluorine content increases. Moreover, the secondary γ relaxation is also faster in the fluorinated networks, and shows a clear decrease of the activation energy with increasing fluorination. The time scale of the secondary β relaxation is also affected in the same way, while the activation energy is constant in the analyzed temperature and frequency range. These experimental results could be rationalized in terms of an increase of the free volume, arising from loosened molecular packing of the chains due to the presence of the flexible FED units and their covalent bonding to the network. Figure 11 shows a scheme of the fluorinated network and the free volume originated by the above mentioned pending chains. These flexible pending chains also affect the network fragility (*m*),^{9,24-26} which decreases as the fluorine content increases (see Table II).

$$m = \frac{DT_0}{T_{g100s} \ln(10)} \left(1 - \frac{T_0}{T_{g100s}} \right)^{-2} \quad (4)$$

The fragility characterizes the deviation of the temperature dependence of the relaxation time from an Arrhenius behavior. Therefore, a system with a non-Arrhenius temperature dependence of its relaxation time close to T_g is called “fragile.”³⁵ In other words, as the fluorine content increases the materials tend to present a very abrupt change in their physical properties as the temperature approaches T_g (whereas less fluorinated materials undergo a relatively smooth transition from the rubbery state to the glassy state). This trend has also been observed for the Jeff-JMF fragilities (see Table I).

Despite the huge change induced in the surface properties,⁴⁻⁶ the chemical modification of the networks progressively increases their bulk mobility, thus reducing their crosslink density, glass transition temperature and fragility. To prevent these undesired side effects, but at the same time keeping a relatively large enrichment of the fluorine surface concentration,¹² chemical modifications of about 1 wt % F appear as the most recommendable option. By keeping the fluorine content close to these concentrations, it is possible to achieve materials with almost the same bulk behavior as the neat and relatively large hydrophobicity (the *F/C* ratio on the materials surface as a function of the *F* wt % is shown in Supporting Information Figure S3).

CONCLUSIONS

Fluorinated epoxy materials were characterized in terms of their calorimetric and dielectric relaxation behavior to determine the effect of the chemical modification on its bulk dynamics. Dielectric processes were successfully identified and it was demonstrated that the fluorinated pendant chains contribute to decrease both the segmental and the secondary relaxation times and to decrease the activation energy of the secondary γ relaxation. A map of the dielectric processes over a concentration range from 0 to 5 wt % showed that up to 1 wt % of fluorine can be introduced in the epoxy networks with a remarkable benefit in the surface properties and no significant weakening of the bulk mechanical behavior.

ACKNOWLEDGMENTS

The authors acknowledge the financial support provided by the Basque Country Government (IT-654-13) and the Spanish Ministry of Science and Innovation (MAT2012-31088). Financial support from EU-funded “European soft matter infrastructure” (Reference 262348 ESMI) is also acknowledged.

REFERENCES

1. Brostow, W.; Cassidy, P. E.; Hagg, H. E.; Jaklewicz, M.; Montemartini, P. E. *Polymer* **2001**, *42*, 7971.
2. van de Grampel, R. D.; Ming, W.; van Gennip, W. J. H.; van der Velden, F.; Laven, J.; Niemantsverdriet, J. W.; van der Linde, R. *Polymer* **2005**, *46*, 10531.

3. Penoff, M. E.; Papagni, G.; Yañez, M. J.; Montemartini, P. E.; Oyanguren, P. A. *J. Polym. Sci. Part B: Polym. Phys.* **2007**, *45*, 2781.
4. Miccio, L. A.; Fasce, D. P.; Schreiner, W. H.; Montemartini, P. E.; Oyanguren, P. A. *Eur. Polym. J.* **2010**, *46*, 744.
5. Miccio, L. A.; Liaño, R.; Schreiner, W. H.; Montemartini, P. E.; Oyanguren, P. A. *Polymer* **2010**, *51*, 6219.
6. Miccio, L. A.; Liaño, R.; Montemartini, P. E.; Oyanguren, P. A. *J. Appl. Polym. Sci.* **2011**, *122*, 608.
7. Penoff, M.; Schreiner, W.; Oyanguren, P.; Montemartini, P. *Macromol. Symp.* **2012**, *321–322*, 186.
8. Genzer, J.; Sivaniah, E.; Kramer, E. J.; Wang, J.; Körner, H.; Xiang, M.; Char, K.; Ober, C. K.; DeKoven, B. M.; Bubeck, R. A.; Chaudhury, M. K.; Sambasivan, S.; Fischer, D. A. *Macromolecules* **2000**, *33*, 1882.
9. Kremer, F.; Schönhals, A. *Broadband Dielectric Spectroscopy*; Springer-Verlag: New York, **2003**.
10. Kummali, M. M.; Alegría, A.; Miccio, L. A.; Colmenero, J. *Macromolecules* **2013**, *46*, 7502.
11. Kummali, M. M.; Miccio, L. A.; Schwartz, G. A.; Alegría, A.; Colmenero, J.; Otegui, J.; Petzold, A.; Westermann, S. *Polymer (United Kingdom)* **2013**, *54*, 4980.
12. Miccio, L. A.; Kummali, M. M.; Montemartini, P. E.; Oyanguren, P. A.; Schwartz, G. A.; Alegra, N.; Colmenero, J. *J. Chem. Phys.* **2011**, *135*, 6.
13. Miccio, L. A.; Kummali, M. M.; Schwartz, G. A.; Alegría, A.; Colmenero, J. *J. Appl. Phys.* **2014**, *115*, 18.
14. Miccio, L. A.; Schwartz, G. A. *AIP Conf. Proc.* **2014**, 1599.
15. Schwartz, G. A.; Riedel, C.; Arinero, R.; Tordjeman, P.; Alegría, A.; Colmenero, J. *Ultramicroscopy* **2011**, *111*, 1366.
16. Fedtke, M. *Makromol. Chem. Macromol. Symp.* **1987**, *7*, 153.
17. Liu, H.; Uhlherr, A.; Varley, R. J.; Bannister, M. K. *J. Polym. Sci. Part A: Polym. Chem.* **2004**, *42*, 3143.
18. Poisson, N.; Lachenal, G.; Sautereau, H. *Vibrat. Spectrosc.* **1996**, *12*, 237.
19. Cole, K. S.; Cole, R. H. *J. Chem. Phys.* **1941**, *9*, 341.
20. Fitz, B.; Andjelić, S.; Mijović, J. *Macromolecules* **1997**, *30*, 5227.
21. Beiner, M.; Ngai, K. L. *Macromolecules* **2005**, *38*, 7033.
22. Kourkoutsaki, T.; Logakis, E.; Kroutilova, I.; Matejka, L.; Nedbal, J.; Pissis, P. *J. Appl. Polym. Sci.* **2009**, *113*, 2569.
23. Havriliak, S.; Negami, S. *J. Polym. Sci. Part C: Polym. Symp.* **1966**, *14*, 99.
24. Vogel, H. *Phys. Z.* **1921**, *22*, 645.
25. Fulcher, G. S. *J. Am. Chem. Soc.* **1925**, *8*, 339.
26. Fulcher, G. S. *J. Am. Chem. Soc.* **1925**, *8*, 789.
27. Woo, M.; Piggott, M. *J. Compos.* **1988**, *10*, 16.
28. Adam, G.; Gibbs, J. H. *J. Chem. Phys.* **1965**, *43*, 139.
29. Povo, F.; Schwartz, G.; Hermida, E. B. *J. Polym. Sci. Part B: Polym. Phys.* **1996**, *34*, 1257.
30. Povo, F.; Hermida, E. B. *J. Appl. Polym. Sci.* **1995**, *58*, 55.
31. Schwartz, G. A.; Cangialosi, D.; Alegría, A.; Colmenero, J. *J. Chem. Phys.* **2006**, *124*, 154904.
32. Cangialosi, D.; Alegría, A.; Colmenero, J. *Phys. Rev. E* **2007**, *76*, 011514.
33. Donth, E. *J. Non-Cryst. Solids* **1982**, *53*, 325.
34. Cervený, S.; Mattsson, J.; Swenson, J.; Bergman, R. *J. Phys. Chem. B* **2004**, *108*, 11596.
35. Kunal, K.; Robertson, C. G.; Pawlus, S.; Hahn, S. F.; Sokolov, A. P. *Macromolecules* **2008**, *41*, 7232.